

Identifying the Hydrogenated Planar Tetracoordinate Carbon: A Combined Experimental and Theoretical Study of CaI_4H and CaI_4H^-

Jing Xu,^{§,†,‡,✉} Xinxing Zhang,^{*,†,‡,+} Shuang Yu,[§] Yi-hong Ding,^{*,§} and Kit H. Bowen^{*,‡,✉}

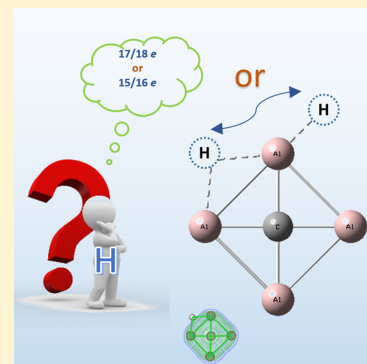
[§]Laboratory of Theoretical and Computational Chemistry, Institute of Theoretical Chemistry, Jilin University, Changchun 130023, People's Republic of China

[†]Noyes Laboratory of Chemical Physics and the Beckman Institute, California Institute of Technology, Pasadena, California 91125, United States

[‡]Department of Chemistry and Department of Material Sciences, Johns Hopkins University, Baltimore, Maryland 21218, United States

Supporting Information

ABSTRACT: The chemical curiosity “planar tetracoordinate carbon” (ptC) has greatly broadened one’s knowledge of molecular bonding motifs apart from the traditional, tetrahedral, van’t Hoff and LeBel’s concept. Synthesized ptC examples have been reported either in the solid state or in the gas phase, where the ptC core is usually metalized or organometallized. Surprisingly, there has been no experimental report on hydrogenated ptC to date. A possible answer to this situation could be the “promiscuity” of hydrogen when binding to other elements, which frustrates the formation of stable ptC that is in competition with other structures. In this Letter, we for the first time identified two hydrogenated ptC species, CaI_4H and CaI_4H^- , based on a photoelectron spectroscopic and quantum chemical study. The favorable site-selectivity of hydrogen was shown to be the bridge of the Al–Al bond rather than the terminus of Al, manifesting the thermodynamic preference of the 17e/18e counting rule over the 15e/16e rule.



Planar tetracoordinate carbon (ptC) has witnessed tremendous advancement in the past 50 years.^{1,2} First proposed by H. J. Monkhorst in 1968,³ the designed planar methane was nevertheless an unstable transition state. Subsequently, Hoffmann et al. proposed two strategies to stabilize ptC,⁴ which have been a general guide to design ptC species. One is the mechanical strategy, which often makes use of transition metals, conjugative rings, or cages to forcibly form ptC. The other is the electronic strategy, which introduces strong σ -donor and π -acceptor ligands or aromatic delocalization to stabilize the p-type lone pair on the ptC center. On the basis of the above two strategies, Schleyer and co-workers theoretically designed the first group of ptC molecules (even though not global minima) in 1976.⁵ Since then, ptC chemistry has been widely developed theoretically^{1,2} and has been extended to planar high-coordinate carbon^{6–8} or planar tetra-/high-coordinate X (X could be other main group elements)^{9–11} as well as the nanosized systems for potential applications in materials science.^{12–14}

In parallel, there have been some experimental investigations on ptC.¹⁵ A class of organometallic ptC has been synthesized in the solid state,¹⁶ but such compounds are usually structurally complicated and involve metals or transition metals as ligands to kinetically stabilize the ptC unit. By contrast, in 1999, a simple penta-atomic ptC cluster CaI_4^- was detected in the gas phase.¹⁷ One year later, several new ptC species, that is, CaI_3Si^- , CaI_3Ge^- , CaI_4^{2-} , and NaCaI_4^- , were characterized.^{18–20} To understand the bonding and stability of these

species, an effective valence electron counting rule, namely, the “18ve-rule”,²¹ has been devised and found applicable in many systems.²² Note that this rule differs sharply from the one mainly associated with compounds composed of transition metal atoms such as $\text{Cr}(\text{C}_6\text{H}_6)_2$ and $\text{Fe}(\text{C}_5\text{H}_5)_2$ where 18 valence electrons are needed to close the s, p, and d shells.^{23–25} Besides, there is an increasing consensus that a ptC structure should have the lowest energy (or be the global minimum) to allow its experimental observation under annealing conditions.²⁶ Moreover, the simplicity of these penta-atomic species has allowed them to act as building blocks for more complicated complexes.^{27–29}

Clearly, in all of the known ptC compounds (except the simplest penta-atomic ptCs), the ptC cores are stabilized by metallic or organometallic ligands. No hydrogenated ptCs have been reported in experiments. By occupying the terminal, bridge or face sites to adjust the skeletal electrons, fascinating hydrogenated topologies can be achieved in compounds such as boranes, alanes, and carboranes.³⁰ A plausible explanation for the absence of hydrogenated ptCs could be the structural fragility of ptC, whose stability highly relies on the subtle balance between the electronic and steric factors. Presumably, being promiscuous in bonding possibilities, hydrogenation

Received: March 27, 2017

Accepted: May 4, 2017

Published: May 4, 2017

would cause undesired competition from other nonplanar structures. In this sense, identifying a global minimum hydrogenated ptC should represent a big challenge for both experiment and theory.

In this Letter, on the basis of anion photoelectron spectroscopy (PES), global structural search, and high-level *ab initio* calculations (see the SI for details), we successfully identified two hydrogenated species, $\text{CAI}_4\text{H}^{-/0}$, both featuring the global minimum ptC. Due to the hydrogen atom's site-selectivity, the observed isomer that fulfills the 17e/18e rule is energetically more favorable than the one with 15e/16e, this being the first time to experimentally prove the preference of 17e/18e ptC over 15e/16e ptC. The present work not only expands the diversity of ptC but more importantly opens a new avenue for hydrogenated ptC chemistry using the tested electronic counting rules.

Experimental details are presented in the SI. Figure 1 presents a typical mass spectrum containing hundreds of

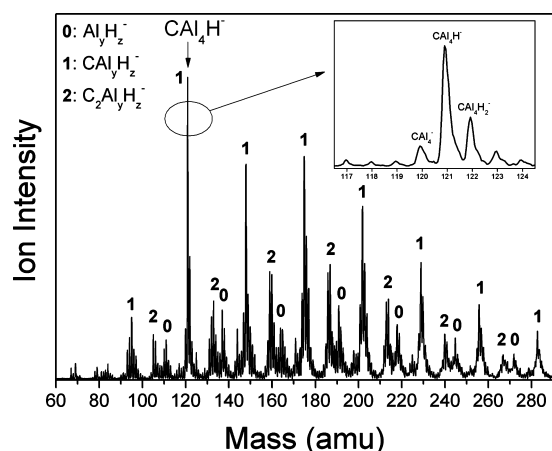


Figure 1. Mass spectrum of the $\text{C}_x\text{Al}_y\text{H}_z^-$ ($x = 0-2$, $y = 1-9$, $z = 1-4$) clusters.

carbon aluminum hydride cluster anions, $\text{C}_x\text{Al}_y\text{H}_z^-$ ($x = 0-2$, $y = 1-9$, $z = 1-4$), and different ion groups are marked by the number of carbon atoms as 0, 1, or 2. Here we highlight only the group with the highest intensity, circled and expanded in Figure 1; it is the CAI_4H_n^- ($n = 0-3$) clusters. Those small peaks to the left of CAI_4^- correspond to the $\text{C}_3\text{Al}_3\text{H}_n^-$ series. By minimizing the carbon powder ratio in the carbon aluminum mixture, we managed to lower the $\text{C}_3\text{Al}_3\text{H}_n^-$ signal as much as possible in order to make sure that $\text{C}_3\text{Al}_3\text{H}_n^-$ did not contaminate the photoelectron spectra of CAI_4H_n^- . In the CAI_4H_n^- ($n = 0-3$) series, CAI_4H^- possesses overwhelmingly higher intensity. It is not only the strongest peak in the neighborhood but also the strongest peak in the entire mass spectrum that contains hundreds of clusters, indicating highly unusual stability of the CAI_4H_1^- cluster. This observation is reasonable in the sense that CAI_4H^- is closed-shell and $\text{CAI}_4\text{H}_{0,2}^-$ are open-shell. However, this conventional wisdom does not apply to CAI_4H_3^- , which is also closed-shell, suggesting that there must be more stabilizing effect contributing to the high intensity of CAI_4H^- (*vide infra*).

When a cluster has a reproducible intense mass spectral peak relative to its neighbors, it is a magic number species. To further investigate this magic cluster CAI_4H^- , we present its photoelectron spectrum in Figure 2, where an electron binding energy (EBE) band starts from 2.6 eV and peaks at 2.88 eV.

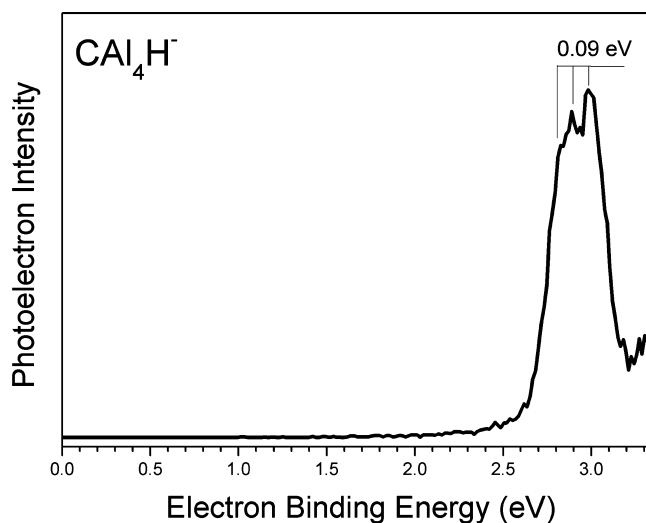


Figure 2. Photoelectron spectrum of the CAI_4H^- cluster.

The experimental electron affinity (EA) of neutral CAI_4H can be determined to be ~ 2.6 eV from the threshold of the spectrum when there is enough Franck–Condon overlap between the anion and the neutral counterpart and when there is not too much hot band present. The experimental vertical detachment energy (VDE) of CAI_4H^- is determined to be the peak position, 2.88 eV, which is the middle one of the three vibrational progressions. This high detachment energy needed for CAI_4H^- again confirms its high stability, consistent with its high mass spectral intensity. The splitting of this EBE band, 0.09 eV, is close to the calculated 725.6 cm^{-1} vibrational mode of the neutral CAI_4H cluster ($\text{CAI}_4\text{H-01}$ at B3LYP/aug-cc-pVTZ level), which is associated with the in-plane swing of the central carbon and ligand hydrogen perpendicular to the Al–Al bond. This is reasonable because the photoelectron is detached from a molecular orbital (MO) that is delocalized within the whole cluster, which causes the bond displacement of the entire skeleton.

The global, unbiased, isomeric search utilizing the “grid” program (see the SI for detail) obtained 32 local minima for CAI_4H^- and 41 local minima for CAI_4H at the level of CBS-QB3. To improve the accuracy, high-level B3LYP/aug-cc-pVTZ (for geometry and vibrational frequencies) and CCSD(T)/aug-cc-pVTZ (for single-point energy) calculations were performed for all of the low-lying isomers ($\Delta E < 10$ kcal/mol at the CBS-QB3 level). Most of the isomers of $\text{CAI}_4\text{H}^{-/0}$ have very high energies; for simplicity, we only show several low-lying isomers in Figure 3. Structures, Cartesian coordinates, and total energies of high-energy isomers can be found in the SI. As seen in Figure 3, $\text{CAI}_4\text{H-01}$ and CAI_4H^-01 featuring a ptC core are the ground-state structures in each system. Unlike CAI_4 and CAI_4^- that have tetrahedral and planar skeletons, respectively, $\text{CAI}_4\text{H-01}$ and CAI_4H^-01 possess very similar skeletons with C_{2v} symmetry; the major difference is that one ligand–ligand bond (Al–Al bond) is broken in the neutral system by removing one electron. The two structures can be viewed as one H-bridge is added to the skeleton of CAI_4^- , forming a H-bridged ptC. Similar H-bridged structures have been found in many boranes and alanes.³⁰ All of the remaining isomers with higher energy in each system have terminal H, among which $\text{CAI}_4\text{H-03}$, $\text{CAI}_4\text{H-04}$, and CAI_4H^-02 also possess ptC structures.

The four C–Al bond lengths and the corresponding Wiberg bond indices (WBIs)³¹ of two ground-state structures are

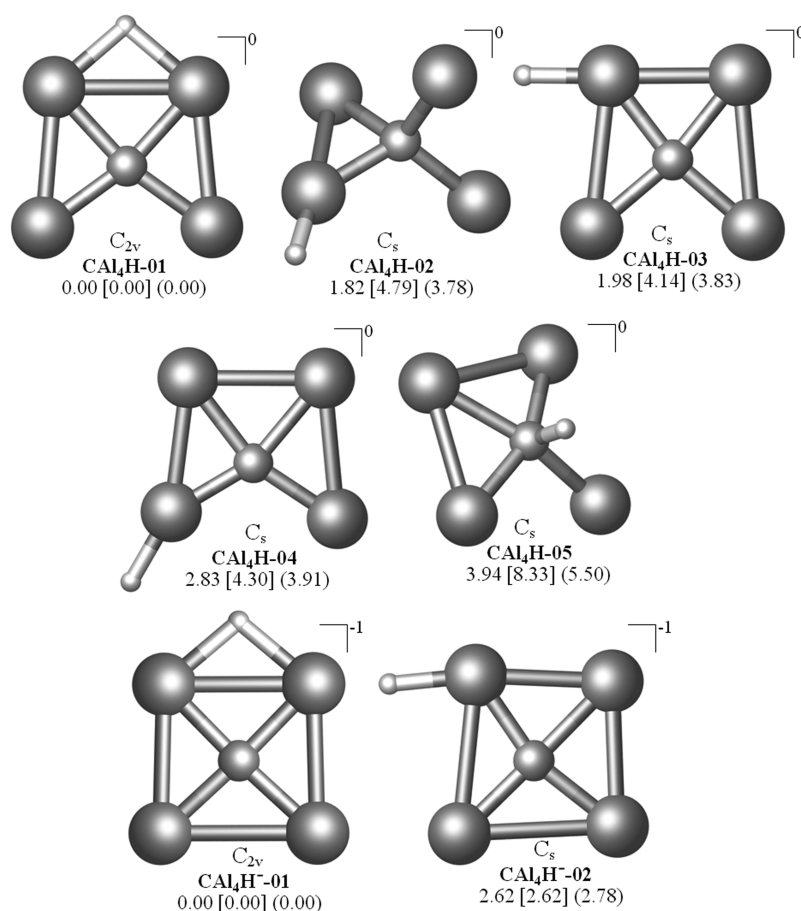


Figure 3. Structures and relative energies (in kcal/mol) of the ground-state and low-lying ptC structures at the CCSD(T)/aug-cc-pVTZ//B3LYP/aug-cc-pVTZ levels of theory. The values in square brackets are at the level of CBS-QB3, and the values in parentheses are at the B3LYP/aug-cc-pVTZ level. All of the energies are corrected by zero-point energy. The energies at the CCSD(T)/aug-cc-pVTZ level were corrected using the zero-point energies obtained at B3LYP/aug-cc-pVTZ.

shown in Figure 4. The C–Al bond lengths range from 1.966 to 2.017 Å, and each $\text{WBI}_{\text{C-Al}}$ is around 0.5. These values indicate

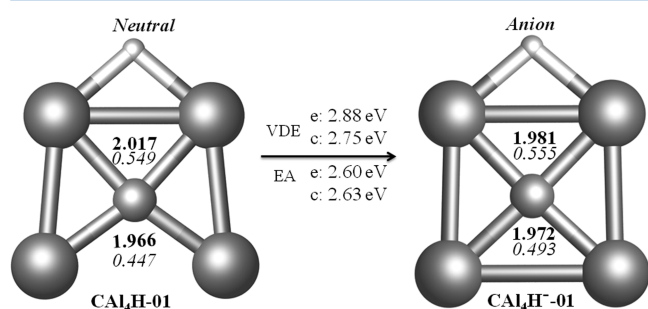


Figure 4. Key structural parameters, WBIs of C–Al bonds, experimental and calculated VDEs, and adiabatic EA of neutral CAL_4H and anion CAL_4H^- ground-state structures. e is short for experiment, and c is short for calculation.

that the bonds between the central C atom and the ligand Al atoms are single bonds. The ptC feature also can be demonstrated from the MOs. In Figure 5, the MOs HOMO–3 (for CAL_4H) and HOMO–4 (for CAL_4H^-) are delocalized π orbitals, which are crucial for achieving the planar geometry and are aromatic. Meanwhile, HOMO–4 (for CAL_4H) and HOMO–3 (for CAL_4H^-) are delocalized ligand–ligand σ -bonding. Addition of one electron reverses

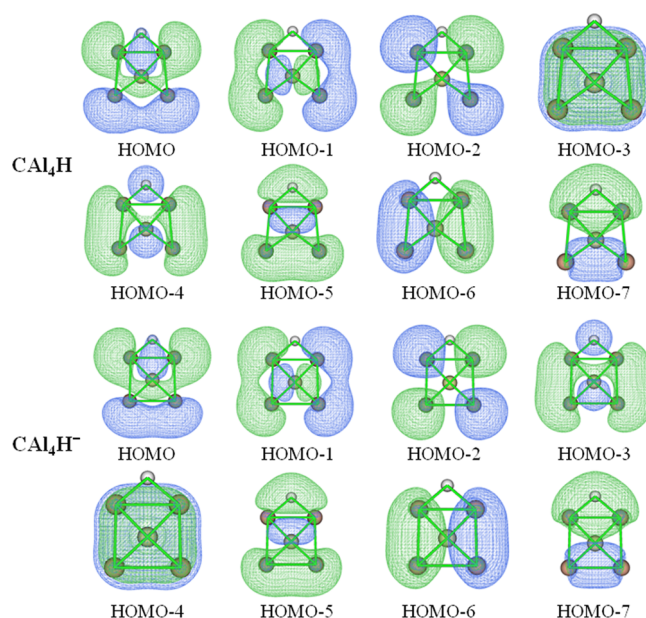


Figure 5. MOs of neutral CAL_4H and anion CAL_4H^- ground-state structures at the level of B3LYP/aug-cc-pVTZ.

the order of delocalized π and σ orbitals. One can observe that the hydrogen is actively hybridized in several MOs (ligand–

ligand and center–ligand), making the electron of hydrogen part of the skeleton. Interestingly, with reference to the 18e- CAL_4^{2-} , the hydrogen in CAL_4H^- strengthens the neighboring Al–Al bonds, whereas Na weakens them in NaCAL_4^- (Figure S1).

To compare with the experiment, the VDE and the adiabatic EA were calculated at the level of CCSD(T)/aug-cc-pVTZ//B3LYP/aug-cc-pVTZ (see Figure 4). The VDE represents the difference in energy between CAL_4H^- in its ground state and neutral CAL_4H having the anion geometry. The EA is the energy difference between the ground states of the neutral and the anionic clusters. Due to the same structure between the neutral ground state and the neutral equilibrium structure with anionic geometry, the EA and adiabatic detachment energy (ADE) have the same values. For the two low-lying isomers of CAL_4H^- , the calculated VDE is 2.75 eV for CAL_4H^- -01 and 2.78 eV for CAL_4H^- -02; both agree well with the experimental 2.88 eV. The calculated EA and ADE are 2.63 eV for CAL_4H^- -01 and 2.60 eV for CAL_4H^- -02, which are also very close to the experimental value of 2.60 eV. However, CAL_4H^- -02, a terminal-H ptC, has a slightly higher energy (around 2 kcal/mol at three different levels) than CAL_4H^- -01 with a H-bridged ptC. We further studied the interconversion between the terminal-H and H-bridged ptC structures. In Figure S2, at the B3LYP/6-311G(2d,d,p) level without zero-point energy correction, the barrier is negligibly small at 0.01 kcal/mol for the neutral system and 0.03 kcal/mol for the anion system. At the sophisticated CBS-QB3 level including zero-point energy correction, the barrier values become slightly negative, which is a reasonable result of computing the higher-level energy at a lower-level geometry. If the Gibbs free energy is concerned, the conversion barriers from the terminal-H ptC to H-bridged ptC structures are 0.67 and 1.33 kcal/mol at 298.15 and 450 K (experimental temperature), respectively. Therefore, the terminal-H structure is very easy to transfer to the H-bridged structure, and coexistence of CAL_4H^- -02 is unlikely in the experiment. The good agreement between theory and experiment indicates that the ground ptC H-bridged ptC states of $\text{CAL}_4\text{H}^{-/0}$ were detected.

On the basis of the above discussion, the most stable CAL_4H -01 and CAL_4H^- -01 are demonstrated as ptC with a bridging H. The hydrogen atom effectively donates its electron to the skeleton by hybridization in several MOs, which is supported by the MOs in Figure 5. Thus, for anionic CAL_4H^- -01 with a bridging-H motif, the skeleton has $4 + 3 \times 4 = 16$ electrons available from the carbon and aluminum atoms, plus 1 electron from the bridged hydrogen atom and 1 electron from negative charge, summing to a total of 18 electrons. Similarly, the neutral CAL_4H -01 has 17 electrons. In the terminal-H motif on the other hand, the Al–H bond consumes two electrons to form a localized σ bond (the occupation number is 1.96 according to NBO calculations), which cannot contribute to the delocalization of the skeleton. Thus, these higher-energy anionic isomers with a terminal H only have 16 electrons available. Accordingly, the higher-energy neutral isomers with a terminal H have 15 electrons, and the MOs are shown in Figure S3. This directly demonstrates that the bridging-H isomers with 17e/18e are more stable than the terminal-H isomers with 15e/16e. While previously studied 17e/18e species mainly comprise the metalized or organometallized ptC cores, the presently identified hydrogenated ptCs have expanded our knowledge on ptC.

In summary, the hydrogenated ptC species CAL_4H and CAL_4H^- have been identified theoretically and experimentally for the first time. They both contain the ptC core with a bridging H as the global minima. The hydrogen atom, even though known to be able to bind to diverse sites, selectively binds to the bridging site in lieu of the terminal sites, demonstrating that the 17e/18e ptCs with bridging H are more stable than 15e/16e ptCs with terminal H, making it a good example of the success of the electron counting rules. Experiment and theory have demonstrated and interpreted the unusual stability of CAL_4H^- , which can be understood by its electronic structures and MOs.

■ ASSOCIATED CONTENT

Supporting Information

The Supporting Information is available free of charge on the ACS Publications website at DOI: 10.1021/acs.jpcllett.7b00732.

Detailed description of the experimental and theoretical methods; structures, total energies, and the Cartesian coordinates of all of the isomers; the barrier between the bridging-H ptC and the terminal-H ptC; and molecular orbitals of the terminal-H ptC (PDF)

■ AUTHOR INFORMATION

Corresponding Authors

*E-mail: zhangx@caltech.edu (X.Z.).

*E-mail: yhdd@jlu.edu.cn (Y.-h.D.).

*E-mail: kbowen@jhu.edu (K.H.B.).

ORCID

Jing Xu: 0000-0001-5558-6908

Kit H. Bowen: 0000-0002-2858-6352

Present Address

[‡]J.X.: Department of Chemistry, University of California, Irvine, CA 92697, USA.

Author Contributions

[†]J.X. and X.Z. contributed equally to this work.

Notes

The authors declare no competing financial interest.

■ ACKNOWLEDGMENTS

The theoretical work was supported by the National Natural Science Foundation of China (No. 21273093, 21473069, 21073074) (Y.-h.D.). This material is based upon work supported by the Air Force Office of Scientific Research (AFOSR), under Grant No. FA9550-15-1-0259 (K.H.B.).

■ REFERENCES

- (1) Keese, R. Carbon Flatland: Planar Tetracoordinate Carbon and Fenestranes. *Chem. Rev.* **2006**, *106*, 4787–4808.
- (2) Yang, L.-M.; Ganz, E.; Chen, Z.; Wang, Z.-X.; Schleyer, P. v. R. Four Decades of the Chemistry of Planar Hypercoordinate Compounds. *Angew. Chem., Int. Ed.* **2015**, *54*, 9468–9501.
- (3) Monkhorst, H. J. Activation Energy for Interconversion of Enantiomers Containing an Asymmetric Carbon Atom without Breaking Bonds. *Chem. Commun.* **1968**, 1111–1112.
- (4) Hoffmann, R.; Alder, R. W.; Wilcox, C. F. Planar Tetracoordinate Carbon. *J. Am. Chem. Soc.* **1970**, *92*, 4992–4993.
- (5) Collins, J. B.; Dill, J. D.; Jemmis, E. D.; Apeloig, Y.; Schleyer, P. v. R.; Seeger, R.; Pople, J. A. Stabilization of Planar Tetracoordinate Carbon. *J. Am. Chem. Soc.* **1976**, *98*, 5419–5427.

- (6) Pei, Y.; An, W.; Ito, K.; Schleyer, P. v. R.; Zeng, X. C. Planar Penta-coordinate Carbon in CA_5^+ : A Global Minimum. *J. Am. Chem. Soc.* **2008**, *130*, 10394–10400.
- (7) Wang, Z.-X.; Schleyer, P. v. R. Construction Principles of “Hyparenes”: Families of Molecules with Planar Penta-coordinate Carbons. *Science* **2001**, *292*, 2465–2469.
- (8) Exner, K.; Schleyer, P. v. R. Planar Hexacoordinate Carbon: A Viable Possibility. *Science* **2000**, *290*, 1937–1940.
- (9) Boldyrev, A. I.; Li, X.; Wang, L.-S. Experimental Observation of Pentaatomic Tetracoordinate Planar Si- and Ge-Containing Molecules: MAI_4^- and MAl_4 . *Angew. Chem., Int. Ed.* **2000**, *39*, 3307–3310.
- (10) Islas, R.; Heine, T.; Ito, K.; Schleyer, P. v. R.; Merino, G. Boron Rings Enclosing Planar Hypercoordinate Group 14 Elements. *J. Am. Chem. Soc.* **2007**, *129*, 14767–14774.
- (11) Menzel, M.; Steiner, D.; Winkler, H.-J.; Schweikart, D.; Mehler, S.; Fau, S.; Frenking, G.; Massa, W.; Berndt, A. Compounds with Planar Tetracoordinate Boron Atoms: Anti van't Hoff/Le Bel Geometries without Metal Centers. *Angew. Chem., Int. Ed. Engl.* **1995**, *34*, 327–329.
- (12) Li, Y.; Liao, Y.; Chen, Z. Be_2C Monolayer with Quasi-Planar Hexacoordinate Carbons: A Global Minimum Structure. *Angew. Chem., Int. Ed.* **2014**, *53*, 7248–7252.
- (13) Li, Y.; Liao, Y.; Schleyer, P. v. R.; Chen, Z. Al_2C Monolayer: The Planar Tetracoordinate Carbon Global Minimum. *Nanoscale* **2014**, *6*, 10784–10791.
- (14) Zhang, Z.; Liu, X.; Yakobson, B. I.; Guo, W. Two-Dimensional Tetragonal TiC Monolayer Sheet and Nanoribbons. *J. Am. Chem. Soc.* **2012**, *134*, 19326–19329.
- (15) Röttger, D.; Erker, G. Compounds Containing Planar-Tetracoordinate Carbon. *Angew. Chem., Int. Ed. Engl.* **1997**, *36*, 812–827.
- (16) Cotton, F. A.; Millar, M. The Probable Existence of A Triple Bond Between Two Vanadium Atoms. *J. Am. Chem. Soc.* **1977**, *99*, 7886–7891.
- (17) Li, X.; Wang, L.-S.; Boldyrev, A. I.; Simons, J. Tetracoordinated Planar Carbon in the Al_4C^- Anion. A Combined Photoelectron Spectroscopy and Ab Initio Study. *J. Am. Chem. Soc.* **1999**, *121*, 6033–6038.
- (18) Wang, L.-S.; Boldyrev, A. I.; Li, X.; Simons, J. Experimental Observation of Pentaatomic Tetracoordinate Planar Carbon-Containing Molecules. *J. Am. Chem. Soc.* **2000**, *122*, 7681–7687.
- (19) Boldyrev, A. I.; Wang, L.-S. Beyond Classical Stoichiometry: Experiment and Theory. *J. Phys. Chem. A* **2001**, *105*, 10759–10775.
- (20) Li, X.; Zhang, H.-F.; Wang, L.-S.; Geske, G. D.; Boldyrev, A. I. Pentaatomic Tetracoordinate Planar Carbon, $[\text{CAI}_4]^{2-}$: A New Structural Unit and Its Salt Complexes. *Angew. Chem., Int. Ed.* **2000**, *39*, 3630–3632.
- (21) Schleyer, P. v. R.; Boldyrev, A. I. A New, General Strategy for Achieving Planar Tetracoordinate Geometries for Carbon and Other Second Row Periodic Elements. *J. Chem. Soc., Chem. Commun.* **1991**, 1536–1538.
- (22) Boldyrev, A. I.; Simons, J. Tetracoordinated Planar Carbon in Pentaatomic Molecules. *J. Am. Chem. Soc.* **1998**, *120*, 7967–7972.
- (23) Langmuir, I. Types of Valence. *Science* **1921**, *54*, 59–67.
- (24) Mitchell, P. R.; Parish, R. V. The Eighteen Electron Rule. *J. Chem. Educ.* **1969**, *46*, 811–814.
- (25) Jensen, W. B. The Origin of the 18-Electron Rule. *J. Chem. Educ.* **2005**, *82*, 28.
- (26) Averkiev, B. B.; Zubarev, D. Y.; Wang, L.-M.; Huang, W.; Wang, L.-S.; Boldyrev, A. I. Carbon Avoids Hypercoordination in CB_6^- , CB_6^{2-} , and C_2B_5^- Planar Carbon–Boron Clusters. *J. Am. Chem. Soc.* **2008**, *130*, 9248–9250.
- (27) Crigger, C.; Wittmaack, B. K.; Tawfik, M.; Merino, G.; Donald, K. J. Plane and Simple: Planar Tetracoordinate Carbon Centers in Small Molecules. *Phys. Chem. Chem. Phys.* **2012**, *14*, 14775.
- (28) Li, S.-D.; Ren, G.-M.; Miao, C.-Q.; Jin, Z.-H. $\text{M}_4\text{H}_4\text{X}$: Hydrometals ($\text{M}=\text{Cu}, \text{Ni}$) Containing Tetracoordinate Planar Nonmetals ($\text{X}=\text{B}, \text{C}, \text{N}, \text{O}$). *Angew. Chem., Int. Ed.* **2004**, *43*, 1371–1373.
- (29) Wu, Y.-B.; Li, Z.-X.; Pu, X.-H.; Wang, Z.-X. Design of Molecular Chains Based on the Planar Tetracoordinate Carbon Unit C_2Al_4 . *J. Phys. Chem. C* **2011**, *115*, 13187–13192.
- (30) Aldridge, S.; Downs, A. J. Hydrides of the Main-Group Metals: New Variations on an Old Theme. *Chem. Rev.* **2001**, *101*, 3305–3366.
- (31) Wiberg, K. B. Application of The Pople-Santry-Segal CNDO Method to the Cyclopropylcarbanyl and Cyclobutyl Cation and to Bicyclobutane. *Tetrahedron* **1968**, *24*, 1083–1096.